Hindawi Publishing Corporation
EURASIP Journal on Wireless Communications and Networking
Volume 2010, Article ID 127657, 9 pages
doi:10.1155/2010/127657

Research Article

On the Capacity of FSO Links over Gamma-Gamma Atmospheric Turbulence Channels Using OOK Signaling

Antonio García-Zambrana,[1] Carmen Castillo-Vázquez,[2] and Beatriz Castillo-Vázquez[1]

[1] *Department of Communications Engineering, University of Málaga, 29071 Málaga, Spain*
[2] *Department of Statistics and Operations Research, University of Málaga, 29071 Málaga, Spain*

Correspondence should be addressed to Antonio García-Zambrana, agz@ic.uma.es

Received 27 November 2009; Accepted 26 March 2010

Academic Editor: Deva K. Borah

A new upper bound on the capacity of power- and bandwidth-constrained optical wireless links over gamma-gamma atmospheric turbulence channels with intensity modulation and direct detection is derived when on-off keying (OOK) formats are used. In this free-space optical (FSO) scenario, unlike previous capacity bounds derived from the classic capacity of the well-known additive white Gaussian noise (AWGN) channel with uniform input distribution, a new closed-form upper bound on the capacity is found by bounding the mutual information subject to an average optical power constraint and not only to an average electrical power constraint, showing the fact that the input distribution that maximizes the mutual information varies with the turbulence strength and the signal-to-noise ratio (SNR). Additionally, it is shown that an increase of the peak-to-average optical power ratio (PAOPR) provides higher capacity values. Simulation results for the mutual information are further demonstrated to confirm the analytical results under several turbulence conditions.

1. Introduction

Optical wireless communications using intensity modulation and direct detection (IM/DD) can provide high-speed links for a variety of applications [1], providing an unregulated spectral segment and high security. Here, the transmit power must be constrained by power consumption concerns and eye-safety considerations. Moreover, these systems are intrinsically bandwidth limited due to the use of large inexpensive optoelectronic components. Recently, the use of atmospheric free-space optical (FSO) transmission is being specially interesting to solve the "*last mile*" *problem*, above all in densely populated urban areas, as well as a supplement to radio-frequency (RF) links [2] and the recent development of radio on free-space optical links (RoFSOLs) [3, 4]. However, atmospheric turbulence produces fluctuations in the irradiance of the transmitted optical beam, which is known as *atmospheric scintillation*, severely degrading the link performance [5, 6].

An upper bound on the capacity of the indoor optical wireless channel was determined in [7] for the specific case of multicarrier systems where the average optical amplitude in each disjoint symbol interval is fixed. By contrast, Hranilovic and Kschischang determine in [8] an upper bound by not assuming a particular signaling set and allowing for the average optical amplitude of each symbol to vary. This upper bound is improved at low signal-to-noise ratio for IM/DD channels with pulse amplitude modulation in [9]. In [10], a new closed-form upper bound on the capacity is found through a sphere-packing argument for channels using equiprobable binary pulse amplitude modulation (PAM) and subject to an average optical power constraint, presenting a tighter performance at lower optical signal-to-noise ratio (SNR) if compared with [8]. Recently, using a dual expression for channel capacity introduced in [11], Lapidoth et al. have derived new upper bounds on the capacity of the indoor optical wireless channel when the input is constrained in both its average and its peak power [12]. In the analysis of the capacity of the atmospheric FSO channel, several works can be cited [13–22]. In [13], numerical results for the capacity of gamma-gamma atmospheric turbulence channels using on-off keying (OOK) formats are presented

by maximizing the mutual information for this channel over a binomial input distribution. In [14, 15], the capacity of log-normal optical wireless channel with OOK formats is computed for known channel state information (CSI) in a similar way to the capacity of the well-known additive white Gaussian noise (AWGN) channel with binary phase shift keying (BPSK) signaling, assuming the fact that the input distribution that maximizes mutual information is the same regardless of the channel state. In [16–18], closed-form mathematical expressions for the evaluation of the average channel capacity are presented when log-normal and gamma-gamma models are adopted for the atmospheric turbulence, assuming the same considerations as in [14, 15]. In [19], the availability of CSI and the effects of channel memory on the capacities of FSO communications channels are investigated by adopting an approach as in [14–18], using a definition of SNR proper to RF fading channels where performance depends on the average power of the electrical current, obtained by the conversion from the optical signal. In [20], closed form expressions for the bit-error rate and the outage probability are presented when pointing errors effects are considered. In [21], ergodic capacity is numerically evaluated for turbulence channels with pointing errors using OOK formats. Recently, Farid and Hranilovic have considered in [22] the design of capacity-approaching, nonuniform optical intensity signaling in the presence of average and peak amplitude constraints, presenting a practical algorithm by using multilevel coding followed by a mapper and multistage decoding at the receiver. The analysis of the channel capacity for alternative FSO scenarios has been considered in [23–25].

In this paper, a new upper bound on the capacity of power- and bandwidth-constrained optical wireless links over gamma-gamma atmospheric turbulence channels with intensity modulation and direct detection is derived when OOK formats are used. Because FSO channel is envisioned as the solution to the convectivity bottleneck problem and as a supplement to RF links, the complexity of transmitter and receiver must be low. Therefore, the use of IM/DD links with OOK formats is proposed as a reasonable choice. In this FSO scenario, unlike previous capacity bounds derived from the classical capacity formula corresponding to the electrical equivalent AWGN channel with uniform input distribution, a new closed-form upper bound on the capacity is found by bounding the mutual information subject to an average optical power constraint and not only to an average electrical power constraint, being considered in our system model the impact of a nonuniform input distribution. This new approach is based on the fact that a necessary and sufficient condition between average optical power and average electrical power constraints is satisfied for OOK signaling where an unidimensional space is assumed with one of the two points of the constellation taking the value of 0, corroborating the nonnegativity constraint. This bound presents a tighter performance at lower optical SNR if compared with previously reported bounds and shows the fact that the input distribution that maximizes the mutual information varies with the turbulence strength and the SNR. Additionally, it is shown that an increase of the peak-to-average optical power ratio (PAOPR) provides higher capacity values. Simulation results for the mutual information are further demonstrated to confirm the analytical results under several turbulence conditions.

2. Atmospheric Turbulence Channel Model

The use of infrared technologies based on IM/DD links is considered, where the instantaneous current in the receiving photodetector, $y(t)$, can be written as

$$y(t) = \eta i(t)x(t) \otimes h(t) + z(t) = x_{\mathrm{rx}}(t) + z(t), \tag{1}$$

where the $\otimes$ symbol denotes convolution, η is the detector responsivity, assumed hereinafter to be the unity, $X \triangleq x(t)$ represents the optical power supplied by the source, $h(t)$ the impulse response of an ideal lowpass filter, which cuts out all frequencies greater than W hertz, modelling the fact that these systems are intrinsically bandwidth limited due to the use of large inexpensive optoelectronic components, and $I \triangleq i(t)$ the scintillation at the optical path; $Z \triangleq z(t)$ is assumed to include any front-end receiver thermal noise as well as shot noise caused by ambient light much stronger than the desired signal at detector. In this case, the noise can usually be modeled to high accuracy as AWGN with zero mean and variance $N_0/2$, that is, $Z \sim N(0, N_0/2)$, independent of the on/off state of the received bit [1]. Since the transmitted signal is an intensity, X must satisfy for all t $x(t) \geq 0$. Due to eye and skin safety regulations, the average optical power is limited and, hence, the average amplitude of X is limited. Although limits are placed on both the average and peak optical power transmitted, in the case of most practical modulated optical sources, it is the average optical power constraint that dominates [26]. The received electrical signal $Y \triangleq y(t)$, however, can assume negative amplitude values. In this fashion, the atmospheric turbulence channel model consists of a multiplicative noise model, where the optical signal is multiplied by the channel irradiance. Here, we consider the gamma-gamma turbulence model proposed in [5, 27], where the normalized irradiance I is defined as the product of two independent random variables, that is, $I = I_x I_y$, I_x and I_y representing large-scale and small-scale turbulent eddies and each of them following a gamma distribution. This leads to the so-called gamma-gamma distribution, whose probability density function (PDF) is given by

$$f_I(i) = \frac{2(\alpha\beta)^{(\alpha+\beta)/2}}{\Gamma(\alpha)\Gamma(\beta)} i^{((\alpha+\beta)/2)-1} K_{\alpha-\beta}\left(2\sqrt{\alpha\beta i}\right), \tag{2}$$

where $\Gamma(\cdot)$ is the well-known Gamma function, and $K_\nu(\cdot)$ is the νth-order modified Bessel function of the second kind [28]. Assuming spherical wave propagation, the parameters

α and β are related to the atmospheric conditions through the following expressions [27, 29]:

$$\alpha = \left[\exp\left(\frac{0.49\chi^2}{\left(1+0.18d^2+0.56\chi^{12/5}\right)^{7/6}}\right)-1\right]^{-1},$$
$$\beta = \left[\exp\left(\frac{0.51\chi^2\left(1+0.69\chi^{12/5}\right)^{-5/6}}{\left(1+0.9d^2+0.62d^2\chi^{12/5}\right)^{7/6}}\right)-1\right]^{-1}, \quad (3)$$

where $\chi^2 = 0.5C_n^2k^{7/6}L^{11/6}$ and $d = (kD^2/4L)^{1/2}$. Here, $k = 2\pi/\lambda$ is the optical wave number, λ is the wavelength, D is the diameter of the receiver collecting lens aperture, and L is the link distance in meters. C_n^2 stands for the altitude-dependent index of the refractive structure parameter and varies from $10^{-13}\,\mathrm{m}^{-2/3}$ for strong turbulence to $10^{-17}\,\mathrm{m}^{-2/3}$ for weak turbulence. Since the mean value of this turbulence model is $E[I] = 1$ and the second moment is given by $E[I^2] = (1+1/\alpha)(1+1/\beta)$, the scintillation index (SI), a parameter of interest used to describe the strength of atmospheric fading, is defined as

$$\mathrm{SI} = \frac{E[I^2]}{(E[I])^2} - 1 = \frac{1}{\alpha} + \frac{1}{\beta} + \frac{1}{\alpha\beta}. \quad (4)$$

We consider OOK formats with any pulse shape and reduced duty cycle, allowing the increase of the PAOPR parameter. A new basis function $\phi(t)$ is defined as $\phi(t) = g(t)/\sqrt{E_g}$ where $g(t)$ represents any normalized pulse shape satisfying the nonnegativity constraint, with $0 \le g(t) \le 1$ in the bit period and 0 otherwise, and $E_g = \int_{-\infty}^{\infty} g^2(t)dt$ is the electrical energy. In this way, an expression for the optical intensity can be written as

$$x(t) = \sum_{k=-\infty}^{\infty} a_k \frac{(1/p)\,T_bP_{\mathrm{opt}}}{G(f=0)} g(t-kT_b), \quad (5)$$

where $G(f=0)$ represents the Fourier transform of $g(t)$ evaluated at frequency $f=0$, that is, the area of the employed pulse shape. The random variable (RV) a_k follows a Bernoulli distribution with parameter p, taking the values of 0 for the bit "0" (off pulse) and 1 for the bit "1" (on pulse). From this expression, it is easy to deduce that the average optical power transmitted is P_{opt}. The constellation here defined for the OOK format using any pulse shape consists of two points in a one-dimensional space with an Euclidean distance of $d = (1/p)P_{\mathrm{opt}}\sqrt{T_b\xi}$ where $\xi = T_bE_g/G^2(f=0)$ represents the square of the increment in Euclidean distance due to the use of a pulse shape of high PAOPR, alternative to the classical rectangular pulse. Assuming maximum-likelihood detection and $h(t)$ as the impulse response of an ideal lowpass filter, which cuts out all frequencies greater than W hertz, the electrical power of X_{rx}, signal corresponding to $x_{\mathrm{rx}}(t)$ at the detector output, conditionated to the irradiance, can be written as $P_{\mathrm{el}} = pd^2i^2\theta = (1/p)P_{\mathrm{opt}}^2i^2T_b\xi\theta$ where θ is obtained from

$$\theta = \int_{-W}^{W} \left|\frac{1}{\sqrt{E_g}}G(f)\right|^2 df \quad (6)$$

with $0 < \theta < 1$, representing the fact that the channel under study is constrained to $\kappa = 2WT_b$ degrees of freedom. In this way, the bandwidth constraint in our analysis is subject to the channel and not to the signaling technique, as in [8]. In our opinion, this is closer to the real scenario. It must be noted that the intersymbol interference between successive code words is considered negligible, assuming that this channel is able to support the transmission of at most κ dimensions per symbol. With the aid of the converse to the coding theorem it is easy to show that the intersymbol interference cannot reduce error probability. There is no problem since we can transmit, in principle, only one code word of arbitrarily long duration, showing that arbitrarily small error probabilities can be achieved at any rate less than capacity [30, Section 8.5]. The channel is assumed to be memoryless, stationary, and ergodic, with independent and identically distributed intensity fast fading statistics. Although scintillation is a slow time varying process relative to typical symbol rates of an FSO system, having a coherence time on the order of milliseconds, this approach is valid because temporal correlation can in practice be overcome by means of long interleavers, being usually assumed both in the analysis from the point of view of information theory and error rate performance analysis of coded FSO links [13, 29, 31]. This assumption has to be considered like an ideal scenario where the latency introduced by the interleaver is not an inconvenience for the required application, being interpreted the results so obtained as upper bounds on the system performance. We also consider that the channel state information is available at both transmitter and receiver. In this way, the channel capacity must be considered as a random variable following the gamma-gamma distribution corresponding to the atmospheric turbulence model and, hence, its average value, known as ergodic capacity, will indicate the average best rate for error-free transmission [16–19].

3. Upper Bound on Channel Capacity

Considering the channel capacity as a random variable and perfect CSI available at both transmitter and receiver [14, 32], we can use the theory derived for discrete-time Gaussian channels [33], expressing the ergodic capacity in bits per channel use as

$$C = \max_{p} \int_0^{\infty} I(X;Y \mid i) f_I(i)di, \quad (7)$$

that is, the maximum, over all distributions on the input that satisfy the average optical power constraint at a level P_{opt}, of the conditional mutual information between the input and output, $I(X;Y \mid i)$, averaged over the PDF in (2). It must be noted that unlike the approach followed in [14–18], where the capacity is computed in a similar way to the capacity of the well-known AWGN channel with BPSK signaling, assuming the fact that the input distribution that maximizes mutual information is the same regardless of the channel state, we consider in our system model the impact of a nonuniform input distribution. In this way, the exchange of integration and maximization is not possible because

the channel we consider does not satisfy a compatibility constraint [32], since the input distribution that maximizes mutual information is not the same regardless of the channel state, as also considered in [13, 34, 35].

The constraint in optical domain implies that $E[X_{\mathrm{rx}}^2]$, the second moment of X_{rx}, takes a value of up to P_{el}. Additionally, in our channel model, assuming a unidimensional space where the nonnegativity constraint is satisfied and one of the two points of the constellation takes the value of 0, it is easy to deduce that an average electrical power constraint of P_{el}, and, hence, $E[X^2] \leq P_{\mathrm{el}}/(i^2\theta)$, implies an Euclidean distance as $d = (1/p)P_{\mathrm{opt}}\sqrt{T_b\xi}$ and, hence, an average optical power constraint of P_{opt}. Thus, an average electrical power constraint of P_{el} is necessary and sufficient condition for satisfying an average optical power constraint of P_{opt}. This is only valid for OOK signaling, representing the basis of our work in order to achieve a tighter performance if compared with previously reported bounds. In relation to the equivalent discrete-time channel, it must be emphasized that the transmitted optical signal is represented by the random variable X, the atmospheric turbulence-induced signal is represented by the product XI, and the corresponding signal performed in electrical domain is represented by X_{rx}, being the latter the signal to be finally considered in our analysis. Applying the fact that the Gaussian distribution maximizes the entropy over all distributions with the same variance [33, Theorem 8.6.5], we obtain

$$I(X;Y \mid i) \leq \frac{1}{2}\log_2\left(1+\frac{\sigma_{X_{\mathrm{rx}}}^2}{N_o/2}\right), \tag{8}$$

where $\sigma_{X_{\mathrm{rx}}}^2 = E[(X_{\mathrm{rx}} - E[X_{\mathrm{rx}}])^2]$ and represents the variance of the optical signal detected in electrical domain, resulting in

$$I(X;Y \mid i) \leq \frac{1}{2}\log_2\left(1+\frac{((1/p)-1)P_{\mathrm{opt}}^2 i^2 T_b \xi\theta}{N_o/2}\right). \tag{9}$$

This expression bounds the conditional mutual information of the bandlimited optical intensity channel corrupted by white Gaussian noise with two-sided spectral density of $N_o/2$ watts/Hz and average optical power constraint of P_{opt} watts. Next, assuming that the channel is constrained to κ dimensions and even without maximizing over the input distribution, the channel capacity $C(\gamma, p)$ can be obtained by averaging over the PDF in (2) as follows:

$$\begin{aligned} C(\gamma,p) &\leq \int_0^\infty \frac{1}{2}\log_2\left(1+\left(\frac{1}{p}-1\right)\kappa\xi\theta\gamma^2 i^2\right) f_I(i)\,di \\ &\leq H_B(p), \end{aligned} \tag{10}$$

where $\gamma = P_{\mathrm{opt}}/\sqrt{N_o W}$ is the SNR definition, as in [8, 10], different to the expression used in [14, 16–19], and $H_B(p) = -p\log_2 p - (1-p)\log_2(1-p)$ represents the entropy of the Bernoulli RV a_k in (5), presenting the maximum value achievable because OOK is the signaling technique considered in this analysis. After substituting (2) in (10), we can use Meijer's G-function [28, equation (9.301)], available in standard scientific software packages such as Mathematica and Maple, in order to transform the integral expresion to the form in [36, equation (21)], expressing in (10) the modified Bessel function of the second kind [36, equation (14)] and the logarithm function [36, equation (11)] in terms of Meijer's G-function. Finally, after a simple power transformation of the RV $I_n = I^2$ in order to achieve a linear argument for Meijer's G-function related to the logarithm function and using [36, equation (21)], a closed-form solution for $C(\gamma, p)$ is derived as can be seen in

$$\begin{aligned} C(\gamma,p) \leq{}& \frac{2^{\alpha+\beta-2}/\log(2)}{(2\pi\Gamma(\alpha)\Gamma(\beta))} \\ &\times G_{6,2}^{1,6}\left(\frac{(16(1/p-1)\xi\theta\kappa)\gamma^2}{\alpha^2\beta^2}\,\middle|\, \begin{matrix} 1,1,\dfrac{1-\alpha}{2},\dfrac{2-\alpha}{2},\dfrac{1-\beta}{2},\dfrac{2-\beta}{2} \\ 1,0 \end{matrix}\right). \end{aligned} \tag{11}$$

Knowing that $C(\gamma, p)$ is also upper bounded by the binary entropy $H_B(p)$, the ergodic capacity in bits per channel use is obtained by maximizing $C(\gamma, p)$ over the parameter p as

$$C = \max_p C(\gamma,p). \tag{12}$$

For the sake of easy comparison, we present a closed-form expression in terms of the Meijer's G-function following a similar approach as in works in the same context [16–18]. Nonetheless, it must be commented that Meijer's G-function has to be numerically calculated and, hence, the use of Monte Carlo integration to solve (10) may represent an alternative with less computational load.

4. Numerical Results

We now numerically evaluate mutual information for our channel model using OOK signaling to corroborate the tightness of the previous results. For the sake of simplicity, showing the fact that the input distribution that maximizes the mutual information varies with the turbulence strength and the SNR, the statistical channel model can be rewritten as

$$Y = AXI + Z, \quad X \in \{0,1\},\ Z \sim N(0,1), \tag{13}$$

where $A = (1/p)\gamma\sqrt{\xi\theta\kappa}$. The conditional mutual information $I(X;Y \mid i)$ for this channel is, therefore, derived as can be seen in

$$I(X;Y \mid i) = \sum_{x=0}^{1} P_X(x) \int_{-\infty}^{\infty} f_Y(y \mid x,i) \times \log_2\left(\frac{f_Y(y \mid x,i)}{\sum_{m=0,1} P_X(m) f_Y(y \mid x=m,i)}\right) dy. \quad (14)$$

as in [13, 19, 21], where $P_X(x = 1) = p$, $P_X(x = 0) = 1 - p$, $f_Y(y \mid x = 1,i) = (1/\sqrt{2\pi})\exp(-(y - Ai)^2/2)$, and $f_Y(y \mid x = 0,i) = f_Y(y \mid x = 0) = (1/\sqrt{2\pi})\exp(-y^2/2)$. Then, substituting (14) in (7), the ergodic capacity is numerically obtained after maximizing over p the expectation with respect to the PDF in (2) of the conditional mutual information. This expression is computed using a symbolic mathematics package [37].

4.1. No Atmospheric Turbulence. Firstly, no atmospheric turbulence is considered to show the fact that the input distribution that maximizes the mutual information varies with the SNR. It is easy to deduce from the upper bound in (9) that the channel capacity C_{nt} in the absence of atmospheric turbulence is obtained by maximizing $C_{\text{nt}}(\gamma, p)$ over p, that is, $C_{\text{nt}} = \max_p C_{\text{nt}}(\gamma, p)$, where $C_{\text{nt}}(\gamma, p)$ is

$$C_{\text{nt}}(\gamma,p) \le \frac{1}{2}\log_2\left(1 + \left(\left(\frac{1}{p}\right) - 1\right)\kappa\xi\theta\gamma^2\right) \le H_B(p). \quad (15)$$

At this point, the greater tightness of this upper bound can be corroborated if compared to the approach followed in [14–18], where the capacity is computed in a similar way to the capacity C_{AWGN} of the well-known AWGN channel with BPSK signaling, assuming the fact that the input distribution that maximizes mutual information is the same regardless of the channel state and with a value of $p = 1/2$. With our notation, this capacity C_{AWGN} can be expressed as

$$C_{\text{AWGN}}(\gamma) \le \frac{1}{2}\log_2\left(1 + \left(\frac{1}{p}\right)\kappa\xi\theta\gamma^2\right)\Big|_{p=1/2} = \frac{1}{2}\log_2(1 + 2\kappa\xi\theta\gamma^2). \quad (16)$$

Obtained results for the capacity $C_{\text{nt}}(\gamma, 1/2)$ in (15), with a value of $p = 1/2$, and $C_{\text{AWGN}}(\gamma)$ in (16) are illustrated in Figure 1 when a rectangular pulse shape with duty cycle of 100% is adopted, that is, $\xi = 1$. Here, $\kappa = 2$ and $\kappa = 20$ have been considered and, hence, values of $\theta = 0.9028$ and $\theta = 0.9898$, respectively, are computed in (6) by direct integration in frequency domain using a symbolic mathematics package [37]. For this rectangular pulse shape, it is easy to deduce that $\theta = 2(\pi\kappa\text{Si}(\pi\kappa) + \cos(\pi\kappa) - 1)/(\pi^2\kappa)$, where $\text{Si}(\cdot)$ is the sine integral function [38, equation (5.2.1)]. In this figure, mutual information $I_{\text{nt}}(X;Y)$ is also displayed, being numerically solved in a similar way as in (14) but not yet considering the impact of the atmospheric turbulence. It can be corroborated

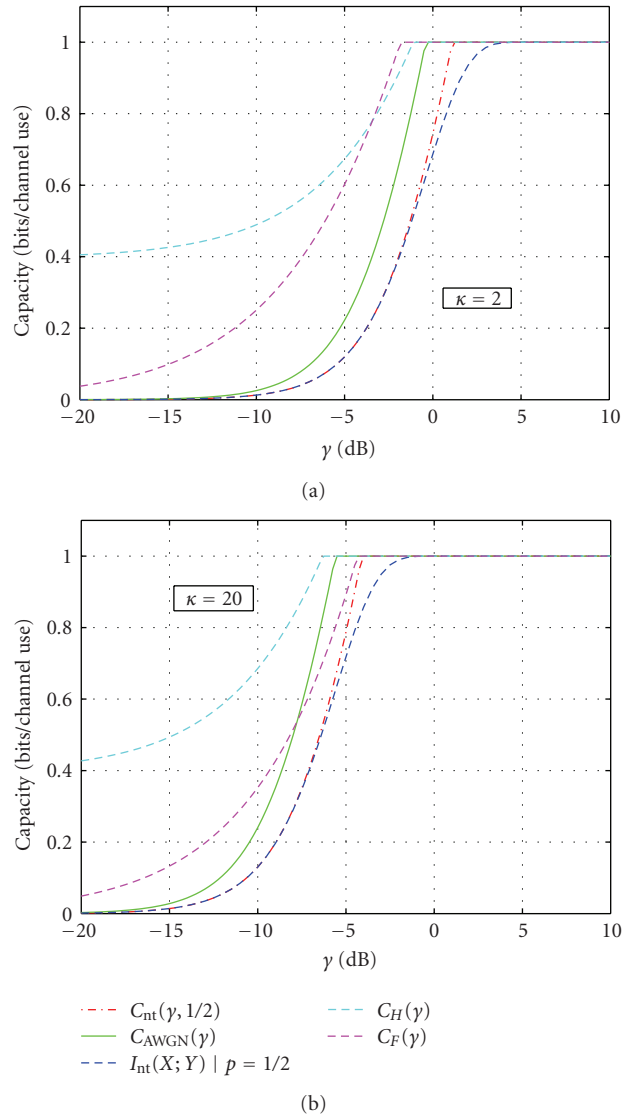

Figure 1: Capacity bounds and mutual information numerically solved for the nonturbulent optical channel with uniform input distribution when a rectangular pulse shape with duty cycle of 100%, that is, $\xi = 1$, and values of (a) $\kappa = 2$ and (b) $\kappa = 20$ are adopted.

that the proposed upper bound in the absence of turbulence $C_{\text{nt}}(\gamma, 1/2)$ shows a tighter performance, regardless of the value of κ. Here, there must be commented the fact that the analysis in this paper is particularized for the OOK signaling and, hence, the improvement in performance for the capacity $C_{\text{nt}}(\gamma, 1/2)$ in (15) is sufficiently contrasted if compared to the mutual information, numerically solved for the OOK signaling. However, when no signaling schemes are particularized in the capacity analysis, upper bounds are usually corroborated by evaluating the asymptotic behavior with the corresponding lower bounds.

In Figure 1, we also include the upper bound on channel capacity determined in [8, expression (21)] by Hranilovic and Kschischang, based on a signal space representing the

convex hull of a generalized N-cone with vertex at the origin. As in [8, Section V.A], this is adopted in the unidimensional case but using the new basis function $\phi(t)$ proposed in this paper to consider the favorable impact of the increase of the PAOPR and, this way, to compare results in similar conditions. It must be noted that the mathematical treatment in [8] is more general since a particular signaling is not assumed when the sphere-packing procedure is carried out. This modified upper bound can be written in bits/channel use as

$$C_H(\gamma) \leq \log_2\left[\left(\sqrt{\kappa\xi\theta\gamma}+2\right)\sqrt{\frac{e}{2\pi}}\right]. \tag{17}$$

Recently, a better representation at lower SNR for the channel capacity (in bits/channel use) has been derived by Farid and Hranilovic in [9, expression (15)], compared to previous work in [8] with

$$C_F(\gamma) \leq \log_2\left[\left(\sqrt{\frac{e^2}{4\pi}}\right)^{\alpha}\left(\sqrt{\kappa\xi\theta\gamma}\right)^{\alpha}\frac{1}{\Theta(\alpha)}\right], \tag{18}$$

where α and $\Theta(\alpha)$ are obtained as explained in [9], depending on SNR values. As a result, the new bound $C_{\text{nt}}(\gamma, 1/2)$ derived in (15) yields superior tightness over the bound in (17) and (18). It can be corroborated that the superiority of the proposed upper bound is even more significant when the value of κ is lower. Recently, using a dual expression for channel capacity introduced in [11], Lapidoth et al. have derived new upper bounds on the capacity of the indoor optical wireless channel when the input is constrained in both its average and its peak power [12]. They also present results on the asymptotic capacity at low power, showing precise results when an average- and a peak-power constraint are imposed, presenting asymptotic upper and lower bounds whose ratio tends to 1 as the power tends to 0. Nonetheless, this ratio tends to $2\sqrt{2}$ as the power tends to 0 when only an average-power constraint is imposed, context in which the upper bound proposed in this paper is evaluated.

Since the input distribution that maximizes the mutual information varies with the SNR, numerical maximization of the capacity bound in (15) and mutual information over the input distribution p for the nonturbulent channel are shown in Figure 2(a) when a rectangular pulse shape with duty cycle of 100%, that is, $\xi = 1$, and $\kappa = 20$ are adopted. Figure 2(b) shows the fact that a nonuniform input distribution improves the channel capacity, especially at low SNR [34, 35]. Unlike other channels in which the gap between mutual information with uniform and nonuniform source distributions is small, this figure demonstrates that for optical wireless systems the use of nonuniform distributions provides a relevant improvement in performance.

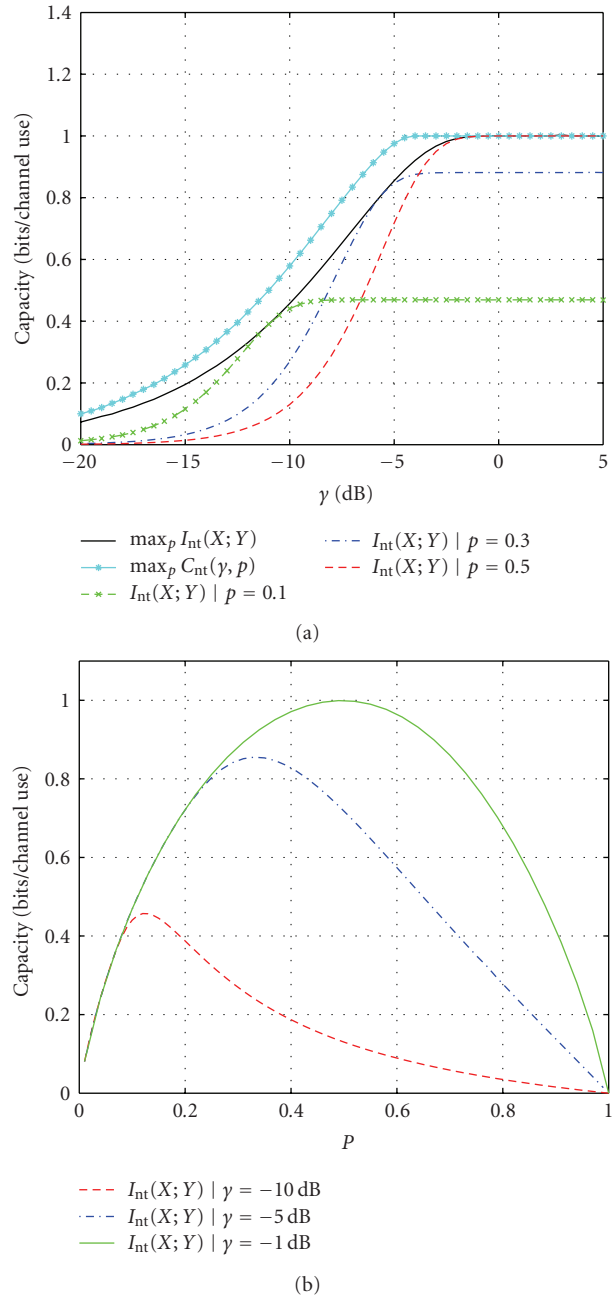

FIGURE 2: (a) Maximization of the capacity bound in (15) and mutual information over the input distribution p for the nonturbulent optical channel when $\kappa = 20$ and a rectangular pulse shape with $\xi = 1$ are adopted. (b) Mutual information versus the input distribution p for values of SNR of $\gamma = -1$ dB, $\gamma = -5$ dB, and $\gamma = -10$ dB.

4.2. With Gamma-Gamma Atmospheric Turbulence. In this subsection, atmospheric turbulence is considered, showing the fact that the input distribution that maximizes the mutual information varies with the turbulence strength and the SNR, and corroborating the better performance for the upper bound in (11) if compared to previous capacity bounds derived from the classic capacity of the well-known AWGN channel with uniform input distribution. In a similar way as derived in (11) but starting from the expression C_{AWGN} in (16), this capacity $C_{\text{AWGN}}^{\text{turb}}$, corresponding to the

approach followed in [14–18], can be written with our notation as can be seen in

$$C_{\mathrm{AWGN}}^{\mathrm{turb}}(\gamma) \leq \frac{2^{\alpha+\beta-2}/\log(2)}{(2\pi\Gamma(\alpha)\Gamma(\beta))} \times G_{6,2}^{1,6}\left(\frac{32\xi\theta\kappa\gamma^2}{\alpha^2\beta^2}\middle| \begin{matrix} 1, 1, \frac{1-\alpha}{2}, \frac{2-\alpha}{2}, \frac{1-\beta}{2}, \frac{2-\beta}{2} \\ 1, 0 \end{matrix}\right). \tag{19}$$

Obtained results for the capacity $C(\gamma, 1/2)$ in (11), with a value of $p = 1/2$, and $C_{\mathrm{AWGN}}^{\mathrm{turb}}(\gamma)$ in (19) are illustrated in Figure 3 when $\kappa = 20$ and a rectangular pulse shape with $\xi = 1$ are adopted. In this figure, mutual information $I(X;Y)$ is also displayed, being numerically solved as in (14). Here, the greater tightness of the proposed upper bound in (11) can be corroborated when a uniform input distribution and different levels of turbulence strength are assumed, corresponding to values of scintillation index of SI = 0.5625 and SI = 1.5.

As in nonturbulent case, since the input distribution that maximizes the mutual information is nonuniform, numerical maximization of the capacity bound in (11) and mutual information over the input distribution p for the gamma-gamma atmospheric turbulent channel are shown in Figure 4(a) when $\kappa = 20$ and a rectangular pulse shape with $\xi = 1$ are used. Figure 4(b) shows the fact that a nonuniform input signaling improves the channel capacity, especially at low SNR [35], depending on the maximizing input distribution on the SNR and the turbulence strength.

Additionally, from the result in (11) for the capacity proposed in this letter, a relevant improvement in performance must be noted as a consequence of the pulse shape used. To fully exploit this improvement, a pulse shape with a high PAOPR must be employed. So, for instance, when a rectangular pulse shape of duration μT_b, with $0 < \mu \leq 1$, is adopted, a value of $\xi = 1/\mu$ can be easily shown. Nonetheless, a significantly higher value of $\xi = 4/\mu\sqrt{\pi}$ is obtained when a Gaussian pulse of duration μT_b as $g(t) = \exp(-t^2/2\sigma^2)$ for all $|t| < \mu T_b/2$ is adopted, where $\sigma = \mu T_b/8$ and the reduction of duty cycle is also here controlled by the parameter μ. In this fashion, 99.99% of the average optical power of a Gaussian pulse shape is being considered. In Figure 5, maximization of the capacity bound in (11) and mutual information for the atmospheric turbulent optical channel are displayed when a scintillation index of SI = 1.5 and rectangular and Gaussian pulse shapes are adopted. Here, a value of $\kappa = 20$ has been considered and, hence, values of $\theta = 0.9898$ when using a rectangular pulse with $\mu = 1$ and $\theta = 0.9945$ when using a Gaussian pulse shape with $\mu = 0.25$ have been obtained from (6). For this Gaussian pulse shape, it is easy to deduce that $\theta = \mathrm{erf}(\pi\kappa\mu/8)$, where $\mathrm{erf}(\cdot)$ is the error function [38, equation (7.1.1)]. It is shown that OOK format using the classical rectangular pulse with duty cycle of 100% requires about 5 dB more optical SNR to yield similar values of capacity compared with OOK format with Gaussian pulses having a duty cycle of 25%.

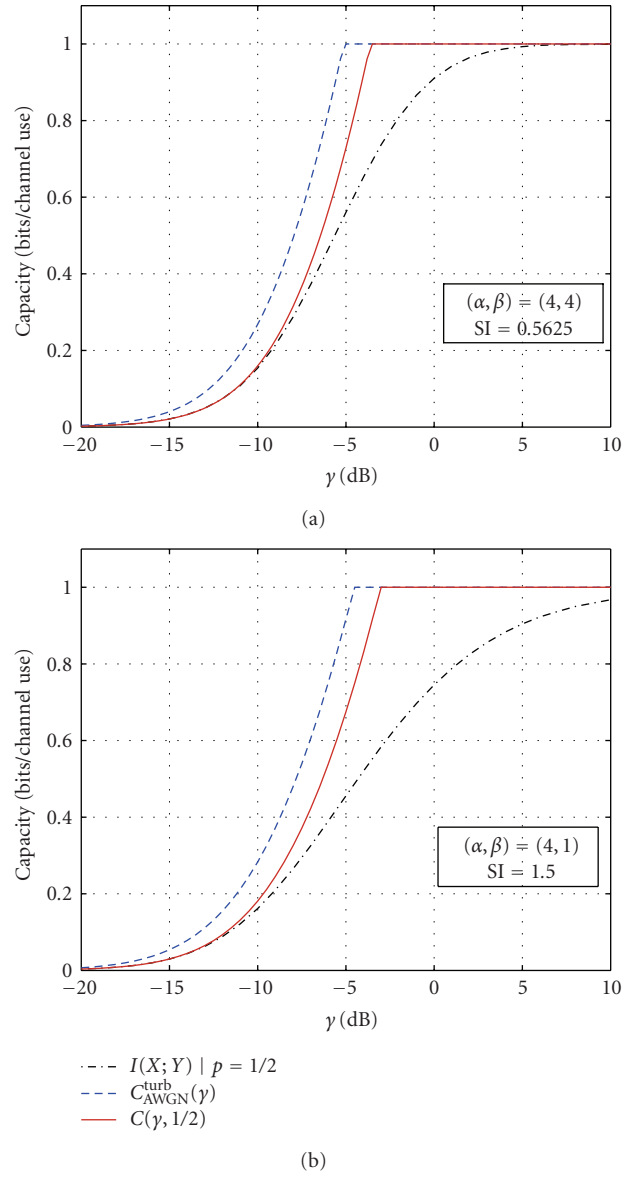

Figure 3: Capacity bounds and mutual information numerically solved for the atmospheric turbulent optical channel with uniform input distribution when $\kappa = 20$, a rectangular pulse shape with $\xi = 1$, and different levels of turbulence strength (a) $(\alpha, \beta) = (4, 4)$ and (b) $(\alpha, \beta) = (4, 1)$ are assumed.

5. Conclusions

As a result, a new upper bound on the capacity of power- and bandwidth-constrained optical wireless links over gamma-gamma atmospheric turbulence channels with intensity modulation and direct detection is derived when OOK formats are used. In this FSO scenario, unlike previous capacity bounds derived from the classic capacity of the well-known AWGN channel with uniform input distribution, a new closed-form upper bound on the capacity is found by bounding the mutual information subject to an average optical power constraint and not only to an average electrical

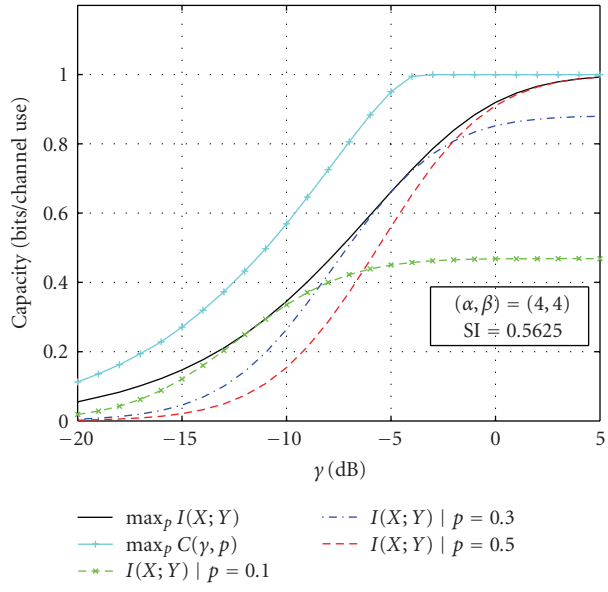

(a)

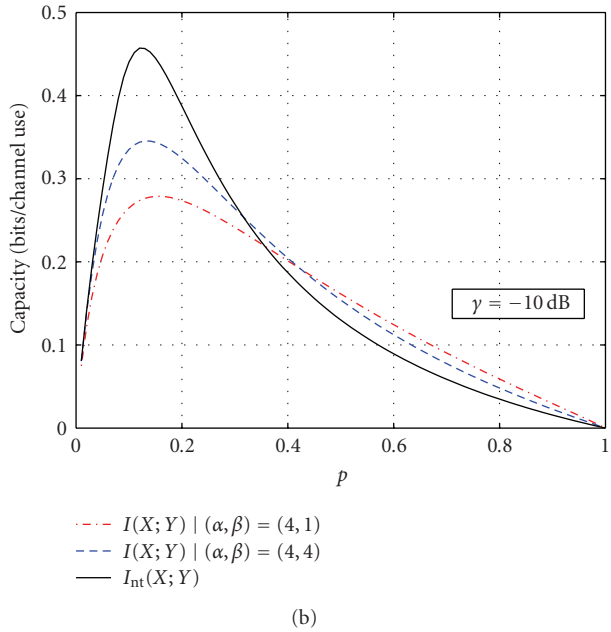

(b)

FIGURE 4: (a) Maximization of the capacity bound in (11) and mutual information over the input distribution p for the atmospheric turbulent optical channel when $\kappa = 20$, a rectangular pulse shape with $\xi = 1$, and a scintillation index of SI = 0.5625 are adopted. (b) Mutual information versus the input distribution p for a value of SNR of $\gamma = -10$ dB and different levels of turbulence strength.

power constraint. This bound presents a tighter performance at lower optical SNR if compared with previously reported bounds and shows the fact that the input distribution that maximizes the mutual information varies with the turbulence strength and the SNR. Additionally, it is shown that an increase of the PAOPR provides higher capacity values. Simulation results for the mutual information are

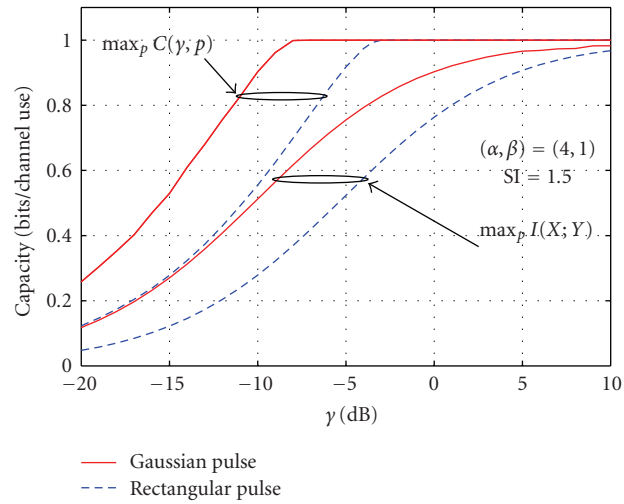

FIGURE 5: Maximization of the capacity bound in (11) and mutual information over the input distribution p for the atmospheric turbulent optical channel when $\kappa = 20$ and a scintillation index of SI = 1.5 are adopted with rectangular and Gaussian pulse shapes.

further demonstrated to confirm the analytical results under different turbulence conditions. From the results here obtained when only an average-power constraint is imposed, investigating the impact of an input constrained in both its average and its peak power as well as misalignment fading on the system model here proposed for representing OOK signaling is an interesting topic for future research.

Acknowledgment

The authors are grateful for financial support from the Junta de Andalucía (research group "Communications Engineering (TIC-0102)").

References

[1] J. M. Kahn and J. R. Barry, "Wireless infrared communications," *Proceedings of the IEEE*, vol. 85, no. 2, pp. 265–298, 1997.

[2] L. B. Stotts, L. C. Andrews, P. C. Cherry, et al., "Hybrid optical RF airborne communications," *Proceedings of the IEEE*, vol. 97, no. 6, pp. 1109–1127, 2009.

[3] W. Lim, C. Yun, and K. Kim, "BER performance analysis of radio over free-space optical systems considering laser phase noise under Gamma-Gamma turbulence channels," *Optics Express*, vol. 17, no. 6, pp. 4479–4484, 2009.

[4] K. Tsukamoto, A. Hashimoto, Y. Aburakawa, and M. Matsumoto, "The case for free space," *IEEE Microwave Magazine*, vol. 10, no. 5, pp. 84–92, 2009.

[5] L. Andrews, R. Phillips, and C. Hopen, *Laser Beam Scintillation with Applications*, SPIE Press, Bellingham, Wash, USA, 2001.

[6] X. Zhu and J. M. Kahn, "Free-space optical communication through atmospheric turbulence channels," *IEEE Transactions on Communications*, vol. 50, no. 8, pp. 1293–1300, 2002.

[7] R. You and J. M. Kahn, "Upper-bounding the capacity of optical IM/DD channels with multiple-subcarrier modulation

and fixed bias using trigonometric moment space method," *IEEE Transactions on Information Theory*, vol. 48, no. 2, pp. 514–523, 2002.

[8] S. Hranilovic and F. R. Kschischang, "Capacity bounds for power- and band-limited optical intensity channels corrupted by Gaussian noise," *IEEE Transactions on Information Theory*, vol. 50, no. 5, pp. 784–795, 2004.

[9] A. A. Farid and S. Hranilovic, "Upper and lower bounds on the capacity of wireless optical intensity channels," in *Proceedings of the IEEE International Symposium on Information Theory (ISIT '07)*, pp. 2416–2420, Nice, France, June 2007.

[10] A. Garcia-Zambrana and B. del Castillo-Vazquez, "Improved upper bound on capacity of optical IM/DD channels using binary pulse amplitude modulation," *Electronics Letters*, vol. 44, no. 12, pp. 760–761, 2008.

[11] A. Lapidoth and S. M. Moser, "Capacity bounds via duality with applications to multiple-antenna systems on flat-fading channels," *IEEE Transactions on Information Theory*, vol. 49, no. 10, pp. 2426–2467, 2003.

[12] A. Lapidoth, S. M. Moser, and M. A. Wigger, "On the capacity of free-space optical intensity channels," *IEEE Transactions on Information Theory*, vol. 55, no. 10, pp. 4449–4461, 2009.

[13] J. A. Anguita, I. B. Djordjevic, M. A. Neifeld, and B. V. Vasic, "Shannon capacities and error-correction codes for optical atmospheric turbulent channels," *Journal of Optical Networking*, vol. 4, no. 9, pp. 586–601, 2005.

[14] J. Li and M. Uysal, "Optical wireless communications: system model, capacity and coding," in *Proceedings of the 58th IEEE Vehicular Technology Conference (VTC '03)*, vol. 1, pp. 168–172, Orlando, Fla, USA, October 2003.

[15] J. Li and M. Uysal, "Achievable information rate for outdoor free space optical communication with intensity modulation and direct detection," in *Proceedings of the IEEE Global Telecommunications Conference (GLOBECOM #39;03)*, vol. 5, pp. 2654–2658, San Francisco, Calif, USA, 2003.

[16] H. G. Sandalidis and T. A. Tsiftsis, "Outage probability and ergodic capacity of free-space optical links over strong turbulence," *Electronics Letters*, vol. 44, no. 1, pp. 46–47, 2008.

[17] H. E. Nistazakis, E. A. Karagianni, A. D. Tsigopoulos, M. E. Fafalios, and G. S. Tombras, "Average capacity of optical wireless communication systems over atmospheric turbulence channels," *Journal of Lightwave Technology*, vol. 27, no. 8, pp. 974–979, 2009.

[18] H. E. Nistazakis, T. A. Tsiftsis, and G. S. Tombras, "Performance analysis of free-space optical communication systems over atmospheric turbulence channels," *IET Communications*, vol. 3, no. 8, pp. 1402–1409, 2009.

[19] S. Z. Denic, I. Djordjevic, J. Anguita, B. Vasic, and M. A. Neifeld, "Information theoretic limits for free-space optical channels with and without memory," *Journal of Lightwave Technology*, vol. 26, no. 19, pp. 3376–3384, 2008.

[20] H. G. Sandalidis, "Optimization models for misalignment fading mitigation in optical wireless links," *IEEE Communications Letters*, vol. 12, no. 5, pp. 395–397, 2008.

[21] D. K. Borah and D. G. Voelz, "Pointing error effects on free-space optical communication links in the presence of atmospheric turbulence," *Journal of Lightwave Technology*, vol. 27, no. 18, pp. 3965–3973, 2009.

[22] A. Farid and S. Hranilovic, "Channel capacity and non-uniform signalling for free-space optical intensity channels," *IEEE Journal on Selected Areas in Communications*, vol. 27, no. 9, pp. 1553–1563, 2009.

[23] S. M. Haas and J. H. Shapiro, "Capacity of wireless optical communications," *IEEE Journal on Selected Areas in Communications*, vol. 21, no. 8, pp. 1346–1357, 2003.

[24] A. Belmonte and J. M. Kahn, "Capacity of coherent free-space optical links using atmospheric compensation techniques," *Optics Express*, vol. 17, no. 4, pp. 2763–2773, 2009.

[25] A. Belmonte and J. M. Kahn, "Capacity of coherent free-space optical links using diversity-combining techniques," *Optics Express*, vol. 17, no. 15, pp. 12601–12611, 2009.

[26] S. Hranilovic and F. R. Kschischang, "Optical intensity-modulated direct detection channels: signal space and lattice codes," *IEEE Transactions on Information Theory*, vol. 49, no. 6, pp. 1385–1399, 2003.

[27] M. A. Al-Habash, L. C. Andrews, and R. L. Phillips, "Mathematical model for the irradiance probability density function of a laser beam propagating through turbulent media," *Optical Engineering*, vol. 40, no. 8, pp. 1554–1562, 2001.

[28] I. S. Gradshteyn and I. M. Ryzhik, *Table of Integrals, Series and Products*, Academic Press, New York, NY, USA, 7th edition, 2007.

[29] M. Uysal, J. Li, and M. Yu, "Error rate performance analysis of coded free-space optical links over gamma-gamma atmospheric turbulence channels," *IEEE Transactions on Wireless Communications*, vol. 5, no. 6, pp. 1229–1233, 2006.

[30] R. G. Gallager, *Information Theory and Reliable Communications*, John Wiley & Sons, New York, NY, USA, 1968.

[31] I. B. Djordjevic, S. Denic, J. Anguita, B. Vasic, and M. A. Neifeld, "LDPC-coded MIMO optical communication over the atmospheric turbulence channel," *Journal of Lightwave Technology*, vol. 26, no. 5, pp. 478–487, 2008.

[32] A. J. Goldsmith and P. P. Varaiya, "Capacity of fading channels with channel side information," *IEEE Transactions on Information Theory*, vol. 43, no. 6, pp. 1986–1992, 1997.

[33] T. M. Cover and J. A. Thomas, *Elements of Information Theory*, John Wiley & Sons, New York, NY, USA, 2nd edition, 2006.

[34] A. A. Farid and S. Hranilovic, "Design of non-uniform capacity-approachingsignaling for optical wireless intensity channels," in *Proceedings of the IEEE International Symposium on Information Theory (ISIT '08)*, pp. 2327–2331, Toronto, Canada, July 2008.

[35] A. A. Farid and S. Hranilovic, "Outage capacity with non-uniform signaling for free-space optical channels," in *Proceedings of the 24th Biennial Symposium on Communications (BSC '08)*, pp. 204–207, Kingston, Canada, June 2008.

[36] V. S. Adamchik and O. I. Marichev, "Algorithm for calculating integrals of hypergeometric type functions and its realization in reduce system," in *Proceedings of the International Symposium on Symbolic and Algebraic Computation*, pp. 212–224, Tokyo, Japan, 1990.

[37] Wolfram Research, *Mathematica, Version 7.0*, Wolfram Research, Champaign, Ill, USA, 2008.

[38] M. Abramowitz and I. A. Stegun, *Handbook of Mathematical Functions with Formulas, Graphs, and Mathematical Tables*, Dover, New York, NY, USA, 9th edition, 1970.